



A study on the Gas-bearing Miocene Sediments of MESSARA Basin in Crete (Greece) by Using Seismic Reflection, Geochemical and Petrophysical Data

George Panagopoulos^{1,3} · Antonios Vafidis¹ · Pantelis Soupios² · Emmanouil Manoutsoglou¹

Received: 7 November 2021 / Accepted: 17 February 2022 / Published online: 17 March 2022
© The Author(s) 2022

Abstract

The focus on exploiting natural gas resources has been increased in the recent years since it was characterized as the transitional fuel to a net-zero era. Consequently, a reevaluation of the gas resources under a new perspective seems to be logical. Within this context, the gas-bearing Miocene sediments of the Messara basin in Crete (Greece) are discussed in this paper. The gas shows have been first reported during the 1990's, without being thoroughly evaluated. This paper presents the interpretation of eight legacy onshore seismic reflection lines, which led to the construction of the 3D subsurface structural model of the Neogene Messara basin. The seismic data reveals the basin depocenter which accommodates approximately 1500 m of the Miocene sediments. The relationship of the Miocene deposits with the existence of shallow gas is also examined and discussed. New organic geochemical results combined with the published geochemical data are used to discuss the gas generation potential of the Miocene sediments. The porosity and permeability measurements on surface samples are also presented to describe the reservoir characteristics. The integration of the data mentioned above suggests that the Miocene sediments of the Messara basin comprise intervals with adequate organic matter to generate the observed gasses and good reservoir sandstones to accumulate the generated gas. The gas might have been trapped by lateral and vertical facies changes which provide efficient stratigraphic trapping mechanisms.

Keywords Miocene basin · Biogenic gas · Hellenic arc · East mediterranean · Seismic interpretation · Field sampling · Laboratory analysis

1 Introduction

Natural gas is currently considered a transition fuel until the moment of the fossil fuel substitution by the renewable forms of energy [1]. The use of natural gas instead of fossil fuels (coal and oil) is the bridge to reduce CO₂ emissions in the near future, but the fact that the combustion of natural gas still emits CO₂ makes it a temporary solution [2, 3]. Under this perspective and given that the current gas price

has reached historically high levels, the evaluation of both new and already known gas fields or shows, is considered reasonable. Thus, the current study focuses on the biogenic gas-bearing deposits of the Messara basin in Greece as a preliminary step toward this direction.

In the late 1990s, several occurrences of shallow gas-shows were reported while drilling water-wells in the broader area of the Messara basin. This provided a different perspective to the shallow gas potential of the study area. However, no sufficient data exist to evaluate the potential of these occurrences due to the lack of deep wells. In the early 1980s the State Petroleum Company of Greece (DEP) conducted a comprehensive seismic survey in the Messara basin, in the southern part of Central Crete (Fig. 1), South Greece, to explore the hydrocarbon potential of the area. This was the first attempt to investigate the subsurface structure of the basin and any existence of hydrocarbon accumulations. The results of this seismic survey have yet to be published.

✉ George Panagopoulos
gpanagopoulos@isc.tuc.gr

¹ School of Mineral Resources Engineering, Technical University of Crete, 73100 Chania, Greece

² Department of Geosciences, College of Petroleum Engineering & Geosciences, King Fahd University of Petroleum and Minerals-KFUPM, Dhahran, Saudi Arabia

³ Energean Italy SpA, Piazza Sigmund Freud, 1, 20154 Milan, Italy



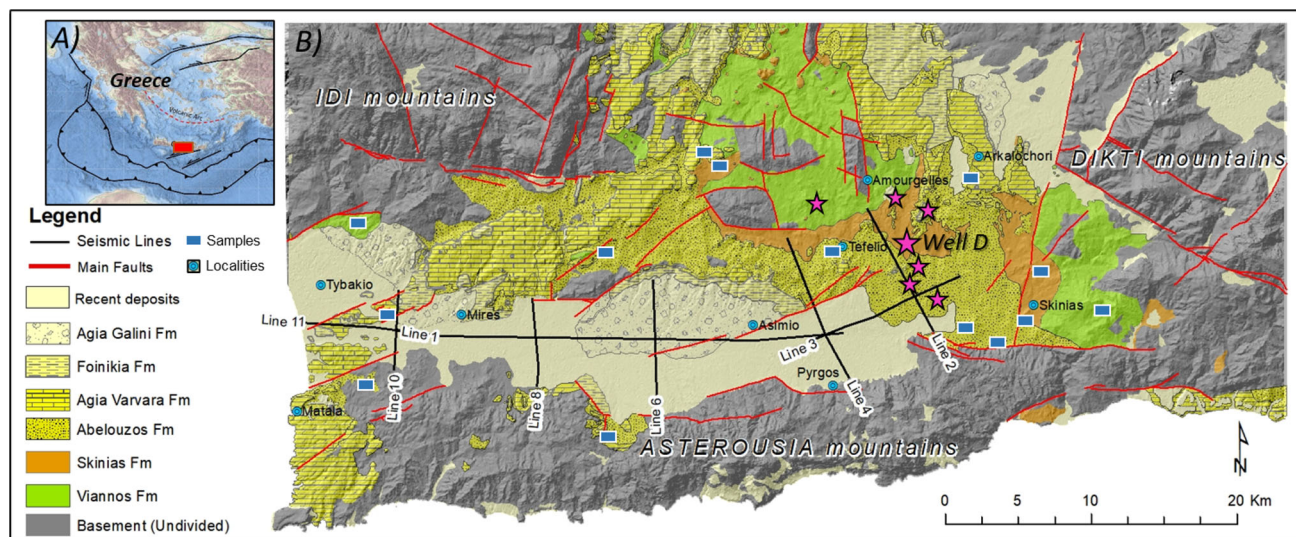


Fig. 1 a Geotectonic position of Crete in the Hellenic Subduction zone (Bathymetry map from EMODnet). b Geological map of the broader Messara area (Compilation of 6 geological sheets 1:50.000 of the Institute of Geology and Mineral Exploration of Greece). The locations of

the available seismic lines are shown in black lines and the sampling locations in blue rectangles. The wells that encountered gas shows are also depicted with purple star symbols

No further investigation has taken place in the basin except for a few recent studies that discuss the area's gas findings based on new geochemical analysis on the Neogene rock samples [4–7]. The current study is the first step to explain the gas occurrences and to examine the gas potential of the Messara basin by integrating existing and new data.

Most of the available data regarding the basin's subsurface structure are related to the hydrogeological potential of the shallower Plio-Quaternary clastic aquifer [8–11]. More than 100 water-wells have been drilled in the Messara basin to exploit the shallow alluvial aquifer [8, data-archive of the Heraklion Prefecture, 2011]. However, the water-wells usually stop at marly horizons of the upper Neogene strata, which are considered aquitards, without reaching the deeper underlying alpine basement. Therefore, the available well-data provides stratigraphic constraints and information only for the shallower Quaternary section.

However, in 2011, the Greek Ministry of Environment and Energy released the eight legacy onshore seismic data acquired in the Messara basin in the early 1980s for scientific research purposes. Vafidis et al. (2012) [12] processed and interpret only one of the seismic lines. In this paper, and for the first time, the entire seismic dataset consisting of eight legacy onshore seismic lines is processed and interpreted. The interpretation of the eight seismic lines gives an insight into the unreachable by the well-data, subsurface in depths basin configuration. Seismic interpretation along with the existing geochemical data and the new porosity and permeability measurements, are integrated to explain the existence of the observed shallow gas.

The results of this study could be used further to evaluate the shallow gas potential of the Messara basin or even as an analogue in terms of source rock and reservoir potential for the Neogene sediments in the adjacent basins. The potential of the Neogene formations to act as good-quality reservoirs has also been identified in the adjacent Ierapetra basin [13]. Such examples prove that new outcrop analogues of extensional basins can be found in other places on Crete that could assist in defining some of the gas exploration elements in similar Miocene basins located in the East Mediterranean region [13].

1.1 Geological Setting

Messara basin is located in Crete Island, Greece, in the Hellenic fore-arc where the African plate subducts the Aegean plate [14–16]. The region is one of the most active seismotectonic areas in Southern Europe, with a convergence rate of 4–5 cm/year [17–20]. The pre-Neogene succession of Crete consists of the Hellenic nappes, which were formed during the Alpine orogeny, stacked over the pre-existing basement. The external Hellenic nappes in Crete consist from bottom to top of the Plattenkalk, Trypali and Phyllite-Quartzite thrust sheets, which are affected by Tertiary HP-metamorphism, and are tectonically overlain by the non-metamorphic Tripolitsa and Pindos thrust sheets [21–23]. The Tripolitsa and Pindos thrust sheets are mainly composed of Mesozoic carbonate rocks covered by Eocene–Oligocene flysch [22]. The pile of stacks is over thrust by the internal Hellenides units of Arvi, Miamou, Vatos, and Asteroussia

[24–27]. The whole pre-Neogene succession is divided into an Upper Sequence of non-metamorphic rocks overlaid the Lower Sequence of metamorphic rocks which are separated by a low-angle detachment fault [21, 30, 31].

The tectonic phase that stacked the successive Alpine sediments into a pile of nappes was the compression until Oligocene. Since Lower Miocene, the tectonic setting changed into largely extensional regime when the HP/LT metamorphic rocks started to exhume [21, 31]. In Late Miocene dominant N-S–striking faults reflect an arc-parallel extension associated with ongoing outward motion of the Aegean arc [32–36]. Along with the extensional regime, structures resulting from left-lateral transpression due to the south-westward motion of the Aegean plate with increasing curvature of the trench are also observed [34, 36]. During Miocene, the extensional phase led to nappe-collapse and exhumation of deep crustal rocks [26, 28, 36, 37]. This event was accompanied by the formation of supra-detachment basins which were filled by Neogene sediments, like the Herakleion basin [36, 38]. The Messara basin was initially part of the wider Herakleion basin, which was then separated from the northern Herakleion basin with the formation of the Central Herakleion Ridge in the Upper Miocene [39].

During the Pliocene–Pleistocene, a series of transpressional and transtensional basins were formed [32, 36, 39–42]. The current geomorphology of Crete has been shaped from the combination of contractional, strike-slip, and extensional tectonic regimes as the result of a syn-convergent extension. Some of them are still active today that uplift the southern Cretan coastline in the area of Messara [44]. The stress pattern for the last 5 Ma supports a combination of left-lateral and right-lateral faulting in Crete along with E-W extension [33]. Today, the Messara basin has a predominant E-W direction, but its geometry is also controlled by a rhombic pattern of 070 and 100 faults [41].

Based on fault plane solutions the recent tectonic regime in the offshore area south of Crete is an NNE–SSW direction of compression [43, 45–48]. On the onshore area, however, an ESE–WNW to roughly N–S extension is predominantly associated with normal and oblique-slip faults. An arc-normal extension is accommodated by ESE–WNW normal fault systems, extending offshore and along with the coastal areas [44, 49]. Arc-parallel extension uniformly affects the entire island generating NNE–SSW normal faults [49].

1.2 Neogene Deposits

The Neogene sediments in the Messara basin have been mainly described by Meulenkaamp et al. (1979) [50]. Zachariasse et al. (2011) [51] propose a slightly different classification (Fig. 2) because the initial classification is inadequate to portray the geological history of the Messara Basin. In this study, the nomenclature of Meulenkaamp et al. (1979) [50] has

been followed since it is the classification that has been used in the official geological sheets prepared by the geological survey of Greece.

The Neogene deposits were deposited in terrestrial to deep marine environments, which indicate significant changes in depositional depths due to the combination of vertical movements and significant climatic changes [36]. A sequence of conglomerates, cobbles, sands, marls, clays and coals was deposited with abrupt lateral and vertical lithological changes. Plant fossil assemblages have been recorded in the Late Serravallian–Early Tortonian and Middle Tortonian sediments [52, 54, 55]. Meulenkaamp et al. [50, 53] subdivided the Neogene sedimentary sequence of Crete into six lithostratigraphic groups (Fig. 2), namely Prina, Tefelion, Vrysses, Hellenikon, Finikia, and Agia Gallini groups. Prina and Hellenikon Groups are absent in the Messara basin. Tefelion has the most extensive coverage, followed by Vrysses Group (Fig. 1, Fig. 2). The Tefelion Group consists of poorly consolidated marine and fluvio-lacustrine conglomerate, sand, silt, and clay uncomfortably overlying the pre-Neogene basement and overlain by limestones and marls (calcareous clays) of the Vrysses Group. The latter consists of marine bioclastic or reefal limestones or alternating laminated and homogeneous marls, which contain evaporite intercalations in some areas [36, 50].

The Tefelion and Vrysses Groups comprise four lithostratigraphic formations, namely the Viannos, Skinias, Ambelouzos, and Agia Varvara formations (Fig. 2) with the latter also including the Messinian evaporites [50]. The Viannos formation comprises a wide range of depositional environments such as channel-belt, overbank and lake deposits. The Skinias formation conformably overlies the Viannos formation and consists of marine clays with interbedded sandstones and occasional gravels [51]. The Ambelouzos formation is the equivalent of the Kasteliana formation, as per the classification suggested by Zachariasse et al. [51], which has been deposited in fluvial-lacustrine, lagoonal and inner neritic environments. The end of the Messinian Crisis is marked by the “Lago Mare” phase and characterized by the fluvio-lacustrine conditions ending the Messinian prior to the marine Pliocene reflooding [38]. The samples that have been studied in this paper are composed of non-consolidated conglomerates, clays, sands representing mainly the Tefelion Group [36] and the marls of the “Lago Mare” deposits [38].

2 Materials and Methods

2.1 Seismic Reflection Data

A seismic reflection survey was conducted in 1982 by the State Petroleum Company (DEP) at the Messara basin to

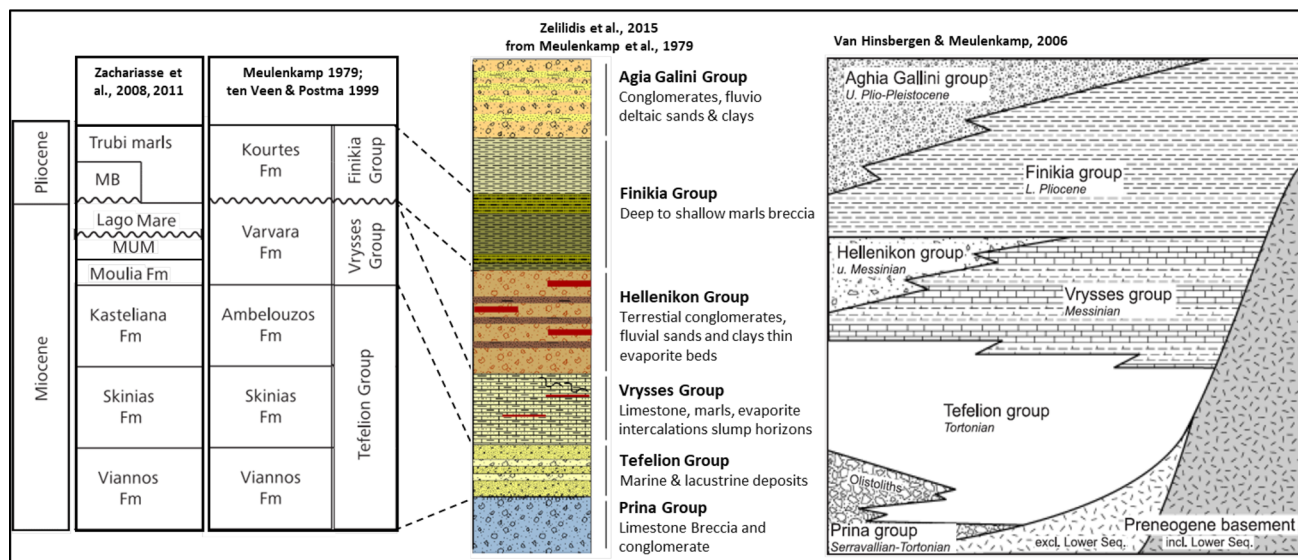


Fig. 2 From left to right: **a** Classification schemes of the Miocene to Pliocene deposits in the Messara basin (modified from [38, 50, 51], supplementary material: MB = Lower Pliocene mass-wasting deposits; MUM = Marine Upper Messinian), **b** General lithostratigraphic column

of the Neogene deposits of Crete [53 modified from 51], **c** Schematic lithostratigraphy of Crete, with the main lithostratigraphic Groups and their vertical and lateral superposition [36]

Table 1 Seismic data acquisition and processing sequence parameters

Acquisition parameters	Source	Dynamite
	Sampling interval	2 ms
	Short interval	100 m
	Number of groups	48
	Near / Far trace	150 m / 1300 m
	Format	SEG-C, 1600
Processing sequence	Demultiplex and gain recovery	
	Resample (4 ms)	
	Anti-aliasing filter (90 Hz cutoff)	
	Trace editing	
	Spherical diverge correction	
	Exponential gain (3 dB/sec)	
	Band-pass filtering	
	Equalization	
	Static correction	
	Deconvolution	
	Dynamic correction	
	Pres-stack mute	
	Velocity analysis	
	Stack	
	Kirchhoff migration	

explore the oil potential. Three east–west and five north–south seismic profiles were acquired to map the pre-Neogene bedrock and further delineate the subsurface basin structure of the area. The reprocessing of those lines and the interpretation of one of the W-E lines, were presented by Vafidis et al. 2012 [12]. Table 1 summarizes the seismic data acquisition and processing flowchart applied. We present in this

study the additional seismic lines of the same survey and their interpretation.

2.2 Geochemical Analysis

The geochemical analysis of 12 samples belonging to the Tefelion Group is presented in this study. The samples were taken from different places of the Messara basin to cover the geographical extend of the Miocene deposits, aiming to give an insight of the biogenic gas potential of the basin in combination to the available published geochemical data. The analysis was performed in the “Laboratory of Hydrocarbons Chemistry and Technology” of the Technical University of Crete. The samples were dried at 100 °C, powdered, and sieved through a 60-mesh sieve before analyzed with the Delsi RockEval-2 following the experimental procedure of Espitalié et al. (1977; 1985). [56, 57].

The procedure gave us the basic pyrolysis indices (Table 2), which are: S_1 (quantity of free hydrocarbons present in the rock sample, mg HC/g rock), S_2 (quantity of heavier hydrocarbons released from pyrolysis, mg HC/g rock), S_3 (CO_2 released from oxygenated compounds during the pyrolysis; mg CO_2 /g rock), T_{max} (the temperature at which the S_2 peak reaches its maximum; °C). Total organic carbon (TOC) (organic richness in a rock by adding the free hydrocarbons and the kerogen; wt%). Hydrogen index (HI) (reflects the quality and quantity of pyrolyzable organic compounds, from S_2 normalized to the TOC; mg HC/g TOC). Oxygen index (OI) (reflects the quantity of terrestrial organic material from

Table 2 Results of the RockEval-2 pyrolysis on the Miocene surface samples from the Messara basin

Sample	Tmax (oC)	S1 (mg/g)	S2 (mg/g)	S3 (mg/g)	TOC (%)	PI	S1 + S2	S2/S3	HI (mg HC/g TOC)	OI (mg CO2/g TOC)	S1/TOC (mg HC/g TOC)
mesi1	463	0.00	0.08	0.45	0.34	0.00	0.08	0.18	24	132	0.00
mesi2	436	0.00	0.11	0.01	0.47	0.00	0.11	11.00	23	2	0.00
mesi3	354	0.00	0.04	0.00	0.21	0.00	0.04	N/A	19	0	0.00
mesi4	–	0.00	0.01	0.00	0.15	0.00	0.01	N/A	7	0	0.00
mesi5	321	0.00	0.02	0.00	0.21	0.00	0.02	N/A	10	0	0.00
mesi7	–	0.00	0.02	0.00	0.18	0.00	0.02	N/A	11	0	0.00
mesi9	413	0.00	0.03	0.31	0.27	0.00	0.03	0.10	11	115	0.00
mesi11	–	0.00	0.00	0.00	0.24	N/A	0.00	N/A	0	0	0.00
dem1	–	0.00	0.02	0.00	0.22	0.00	0.02	N/A	9	0	0.00
dem2	–	0.00	0.01	0.00	0.16	0.00	0.01	N/A	6	0	0.00
am2	426	0.01	0.77	4.67	3.875	0.01	0.78	0.16	20	121	0.00
am9	403	0.00	0.09	1.53	0.35	0.00	0.09	0.06	26	437	0.00
am10	422	0.00	0.12	0.58	0.41	0.00	0.12	0.21	29	141	0.00
am11	419	0.00	0.35	0.70	0.6	0.00	0.35	0.50	58	117	0.00
ski1	419	0.00	0.12	0.67	0.31	0.00	0.12	0.18	39	216	0.00
ski2	419	0.00	0.13	0.59	0.32	0.00	0.13	0.22	41	184	0.00
kas4	386	0.00	0.10	0.16	0.11	0.00	0.10	0.63	91	145	0.00
kas5	360	0.04	0.21	0.38	0.58	0.16	0.25	0.55	36	66	0.07

S3 normalized to TOC; mg CO₂/g TOC. Both parameters define the kerogen type present in the rocks [58–60]. Production index (PI) (the total amount of hydrocarbons (S1 + S2) that may be produced; mg HC/g rock) [61].

2.3 Petrophysical Measurements

There are no publications to describe the petrophysical characteristics of the Miocene sediments of the Messara basin. This study presents the porosity and permeability measurements of Miocene samples taken from different places in the Messara basin in such a way to cover both geographically the entire basin and stratigraphically all the Miocene stratigraphic units (Fig. 1). A 1-inch diameter core plug was extracted from generally loose sandstones for porosity and permeability laboratory measurements. In many cases, the sandstones were too loose to acquire a core plug. The measured values should be therefore regarded as a conservative assessment of the porosity of the Neogene deposits in the Messara basin.

In total, 137 core plugs were acquired. All the core plugs were measured in terms of Helium porosity with the use of Boyle's method, which in a known bulk volume it measures the solids volume of the sample and is used to calculate the pore volume of the sample [62].

For the permeability determination, 25 samples were measured using the steady state method in a Hassler cell. The Hassler apparatus allows to apply different confining pressures on the sample and measuring the air flow across it [62]. The difference in input and output flows is used to calculate the air permeability. The air-permeability was calculated for the same sample by applying three different confining pressure stages, at 25Atm, 100Atm, 200Atm. By this way, the permeability measurement simulates the reservoir conditions that exist in burial depths equivalent to the applied confining pressure. Assuming a typical rock density for the clastics of 2.40 g/cm³, the lithostatic pressure (overburden pressure) for the three different confining pressures corresponds to approximately 100 m, 400 m, and 900 m of burial depth. All the porosity and permeability laboratory measurements were conducted in the “Laboratory of PVT and Core Analysis” of the Technical University of Crete.

3 Results

3.1 Interpretation of Seismic Data

The seismic grid is spread over the Plio-Quaternary cover in the plain part of Messara and extends to the East on the

Neogene sediments (Fig. 1). The pre-Neogene basement surrounds the basin, but no seismic line passes through it, nor any well has penetrated it to be used as a control point for the interpretation. The objective is to interpret the two main stratigraphic horizons in the area, namely the top of Miocene and the top of the Pre-Neogene basement, along with any tectonic feature. Some additional intra-Neogene horizons were picked on seismic only in the eastern part of the basin, where the surface geology enabled us to tie the seismic interpretation.

The interpretation of the Top of the basement was tied to the surface outcrops of these rocks based on the official geological maps [25, 63–66]. The Alpine basement is exposed in the vicinity of the seismic lines. The main tectonic features were depicted along with the top of the basement. Generally, the surface geological maps and the surface topography were the two main datasets that were used to constrain the final interpretation.

The seismic character of both Top of Neogene and Top of the basement horizon were identified. The Top basement horizon is characterized by the continuous strong reflector, which separates the above seismic package of sub-parallel reflections with strong to transparent seismic facies corresponding to the Neogene deposits from the underlying seismic package of mostly chaotic reflections corresponding to the basement.

In the composite seismic line of Fig. 3, the Top of the basement is mostly detected on the central part of the seismic where a continuous strong reflector exists in almost 0.5 s TWT depth. The existence of the Neogene sediments overlaying the basement provides the necessary velocity contrast to map the basement. The geometry of the basement horizon along Line 1 is interpreted as a pop-up structure caused by transpressional tectonics [12]. The eastern part exhibits greater basement depths, as a major normal fault zone has down-thrown the basement to the east. Some deeper reflectors within the basement are due to internal structures originated by the nappe-stacking nature of the basement or/and by the still ongoing exhumation of the metamorphic core complex through the activation of the Cretan low angle detachment fault [29, 36, 51].

In Line 2, the top horizons of two of the Neogene formations (Fig. 4), namely Viannos and Skinias formations have also been interpreted. The interpretation is tied to the surface boundaries of the two formations as mapped on the geological maps of the official geological map [66]. Line 6 shows a structural high in the northern edge of the seismic which can be explained as a result of a transpressional regime, in line with the existence of a similar feature in Line 1. The compressional geometries seen on lines 1 and 2 as having resulted from the transpressional reactivation of basin bounding normal faults, were interpreted.

The rest of the seismic lines (Lines 4, 8, and 10) are of poor quality, making the interpretation challenging (Fig. 5). The main control for interpreting those lines was the interpretation of the intersecting lines and the surface geology. Line 4 covers an area on top of one of the two basement highs that have been identified. Especially to the northern part of the seismic section, the basement is interpreted to be shallow enough to pick on seismic.

The interpretation of the Lines 8 and 10 is tied to the interpretation of intersecting Lines 1 and 11, honoring at the same time the surface faults as mapped on the geological maps of the Institute of Geology and Mineral Exploration of Greece.

The interpretation reveals the maximum depth of the Messara Neogene basin and depicts the thickness variations of the Neogene sediments along the basin. The thickness of the Plio-Quaternary sediments has been calculated on seismic to a maximum of 150 m. This thickness covers approximately the first 0.1 s two-way-traveltime (TWT) on the seismic section in the time domain. The time/depth conversion is based on an average velocity of 2500 m/s which is typical for Plio-Quaternary sediments [67]. Below this depth, the top-Neogene is picked on seismic profiles with high velocities (3000–3500 m/s) especially when the Messinian evaporites are present [67]. There are also parts of the seismic sections that not even the top of the Neogene deposits could be captured efficiently because the Neogene sediments are quite shallow (e.g., depth < 400 m). This is usually also related to a deeper Alpine basement uplift. The Alpine basement shows the greatest velocity contrast to the overburden sediments (velocity > 5000 m/s), which appeared as a strong reflector in the seismic section.

3.2 Gas Occurrences in the Miocene Sediments

Several shallow gas seepages have been reported while drilling water-wells for the irrigation needs of the Messara valley in the past years. The high concentration of methane in these gases indicates a biogenic origin from the Miocene sediments of the Messara basin as suggested by Pasadakis et al. [4]. The so far known water-wells that encountered gas are all located in a narrow zone in the eastern part of Messara basin around well D (Fig. 1), with none of the wells exceeding the 500 m in depth. The generation of the gas and the fairways of gas accumulations are not clear yet, since no complete integrated study has been undertaken so far to evaluate the gas occurrence.

3.2.1 Source Rocks

Biogenic gas is commonly produced in depths shallower than 600 m and temperatures less than 80 °C [68, 69]. However, the existence of deeper biogenic gas accumulations

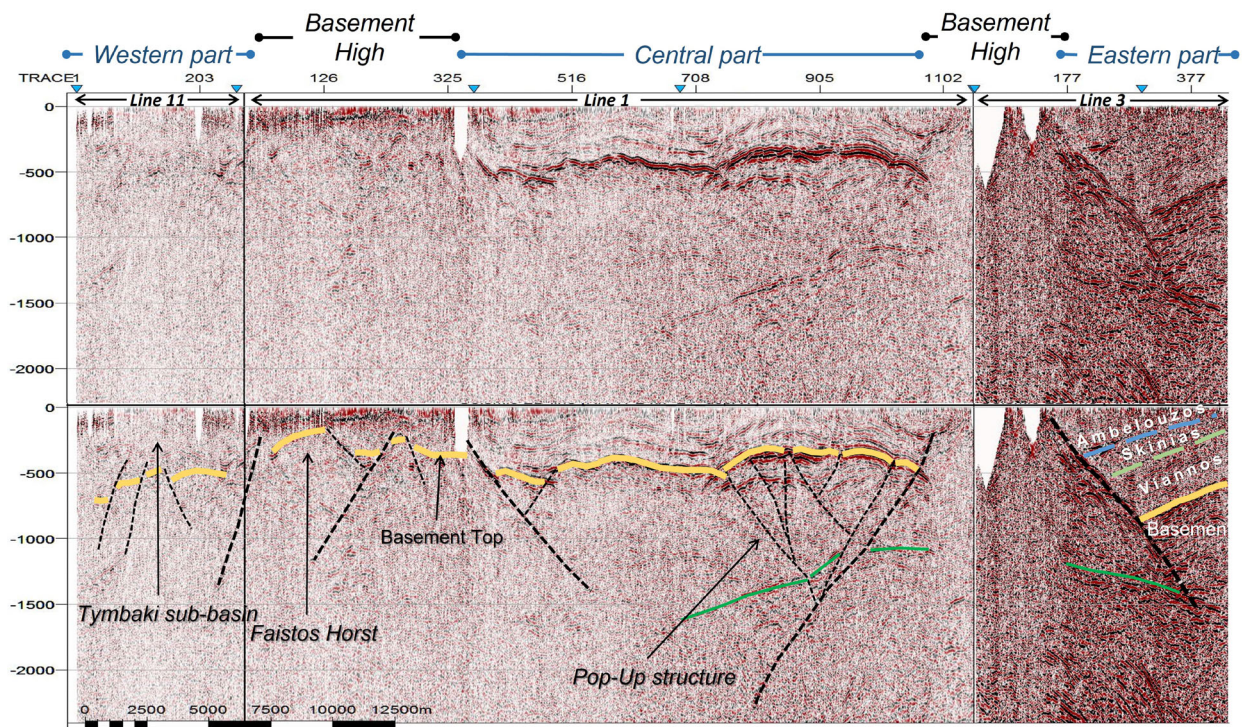


Fig. 3 Composite seismic section of lines 11, 1, and 3 in a direction along the basin (W-E). Main faults (black dashed lines), the basement top (yellow horizon), and a deeper intra-basement reflector (green horizon) are shown. The basin is separated into three distinct parts due to

the existence of two Basement highs. The greater depths are observed in the eastern part, while in the western part, a deepening trend toward the West is observed. The vertical axis in ms TWT

should not be excluded [70]. Biogenic gas accumulations require formations rich in organic matter, anaerobic bacteria to decompose the organic matter, and a trapping mechanism, commonly being of stratigraphic type. Sediments containing greater than 0.2% total organic content (TOC) can potentially generate a free gas phase, which can be trapped if sufficient isolated reservoir intervals are present [69]. Biogenic gas is generally very dry (> 95% methane), contains less than 0.2% ethane [71]. The composition of the gas found in the Miocene sediments of Messara has given approximately 90% methane which indicates a biogenic origin [4–6]. The terrestrial origin of the organic material in the Miocene sediments has been documented either as coal beds [48], or as fossil plant assemblages [52, 54, 55].

A series of geochemical analyses in Miocene sediments of the Messara basin has been conducted in the past to investigate the origin of the gas found in the water-wells [4–7]. The samples were either surface outcrops or ditch cuttings from wells, like well-D shown in Fig. 6. Well-D reached as deep as 450 m providing a representative set of samples of the Miocene succession. According to the results, the samples contain TOC at an average value of 0.45%, while several of them exceed the 0.5% TOC (Fig. 6). The organic matter comes from gas-prone type-III kerogen that has not reached

the oil window. Most of the organic-rich samples belong to Skinias formation and some on the Viannos formation, which are the older Miocene units in the Messara basin [4–6, 50]. The analysis of the samples belonging to the uppermost Miocene succession (Vrysses Group) has also shown the existence of good, type-III kerogen source rocks (up to 2% of TOC) with fair to good hydrocarbon generation potential with an average of 2.1 mg HC/g rock [7].

Similar geochemical studies have been made in the adjacent basins of Crete. In Eastern Crete, Zelilidis et al. [53] presented the geochemical analysis of 14 late Miocene samples in the Sitia basin (Faneromeni formation), and 12 Pliocene samples in the Ierapetra basin (Makrilia formation), which showed a TOC close to 1%. The samples of the Faneromeni formation belong to the Vrysses Group [72] and are time-equivalent to the Messara sediments. Both sample-sets show similarities indicating to the presence of a thermally immature type-III kerogen. In Gavdos island, the organic matter from 53 samples belonging to Metochia formation (Tortonian) was characterized as kerogen type III and IV, with fair potential for gas and/or oil hydrocarbon generation. The TOC-rich samples are found in the lower part of the section with values as high as 2–3%. The studied samples were thermally immature [73].

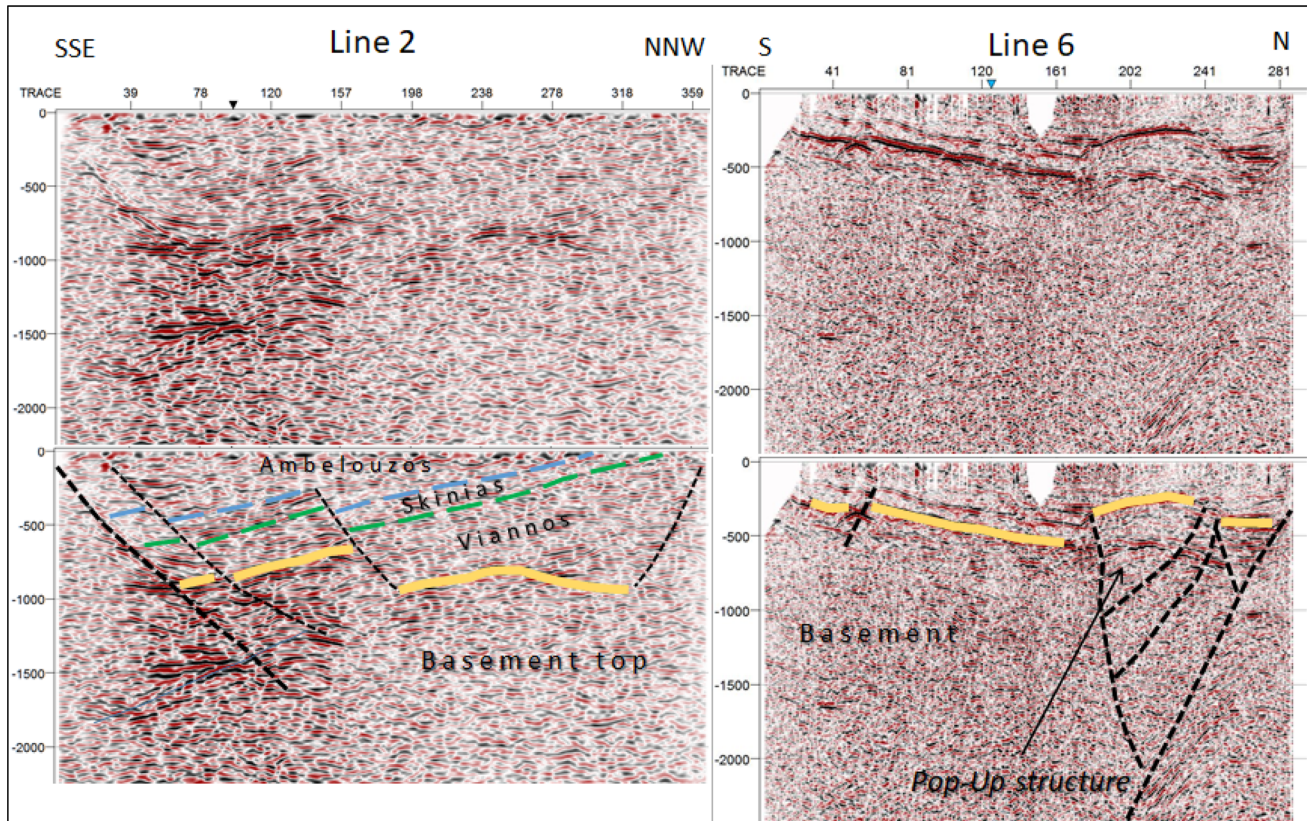


Fig. 4 Line 2 is located in the eastern deeper part of the basin and Line 6 in the central shallower part. The interpretation of the main faults (dashed lines) and the top-horizons of the Basement, the Viannos formation and Skinias formation are shown. The interpretation of the Neogene Top-horizons was controlled only by surface data. The vertical axis in ms TWT

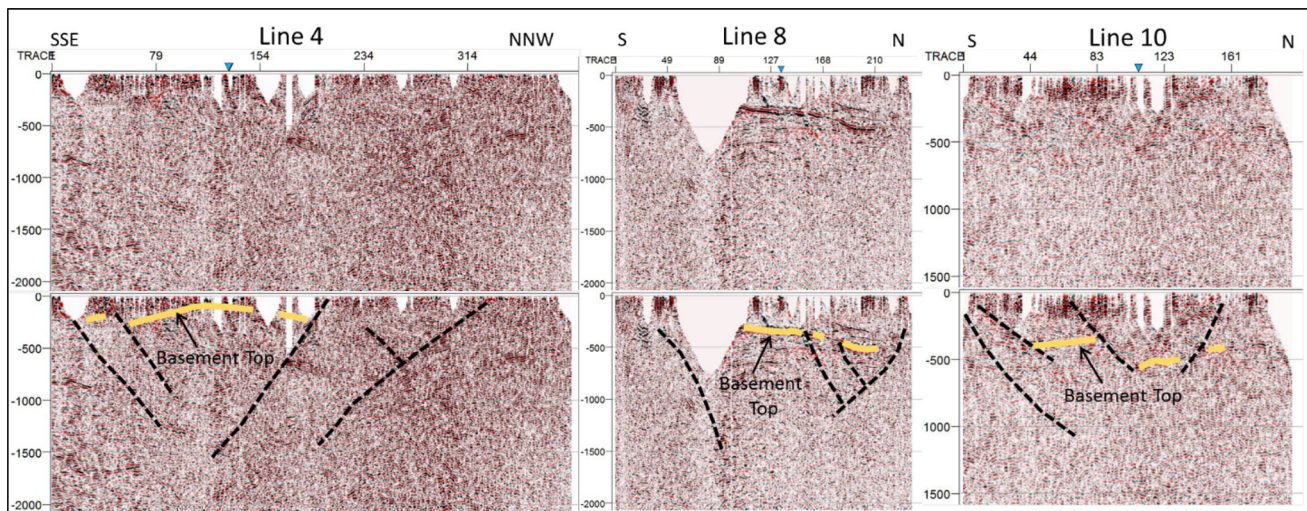


Fig. 5 Seismic interpretation of the basement top in Lines 4, 8 and 10. The quality of those seismic sections was poor. The interpretation was based on the surface geology and the interpretation of the cross-cutting sections. The vertical axis in ms TWT

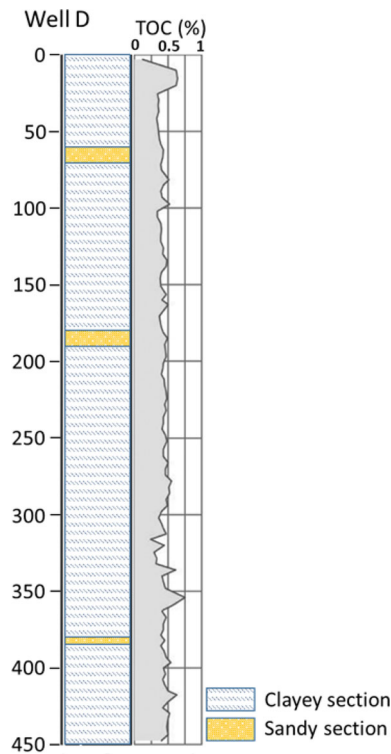


Fig. 6 TOC Rock–Eval results on cuttings from the Well D [5]. The analysis was performed every 4 m-interval. Based on the surface geology, the main part of the well seems to be within the Skinias formation

In this study, the geochemical analysis of 12 samples is presented (Table 2). The TOC values range between 0.1 and 0.6% while one sample reaches 3.9%. The TOC values are low or marginally above the 0.5% TOC cutoff to be characterized as a fair source rock [Fig. 7, 674]. However, TOC

values lower than 0.5% can potentially contribute to biogenic gas generation [5, 75].

The S1 values are close to zero, indicating that the organic matter is still at the early stage of diagenesis. The S2 values are generally low below 1 mg HC/g rock. The Tmax values, which are used as a maturity index of the organic matter [59], indicate generally immature organic matter except for 2 samples that have entered the oil window. Part of the samples is in the gas-prone kerogen area in the van Krevelen diagram (Fig. 7), while the rest of them have oxidized kerogen or show extremely high values of Oxygen Index (OI) which potentially is explained as immature organic material of terrestrial origin [5].

3.2.2 Reservoir Rocks

The sedimentary fill in Messara basin is dominated by continental and shallow marine sediments in the early extension phase, followed by deeper marine deposits as extension continues [50]. The sandstones observed in the basin are mainly found as loose sand to low compacted sandstone, typical of a fluvial/lacustrine environment to a shallow marine [50, 51]. Similar deposits also exist in the adjacent Ierapetra basin. The sediment sorting and the associated porosity are controlled by their distance to the main sediment source areas [13].

The core plugs have been measured in terms of porosity and permeability belong to the three Tefelion stratigraphic Group (Viannos, Skinias and Ambelouzos formations) and the “Lago Mare” deposits. A porosity mean value of 19, 11, 19, and 34% has been calculated out of the 137 samples, respectively (Fig. 8). The Skinias open marine deeper sediments show smaller porosities values compared to the fluvial-lacustrine of the Viannos formation and the shallow

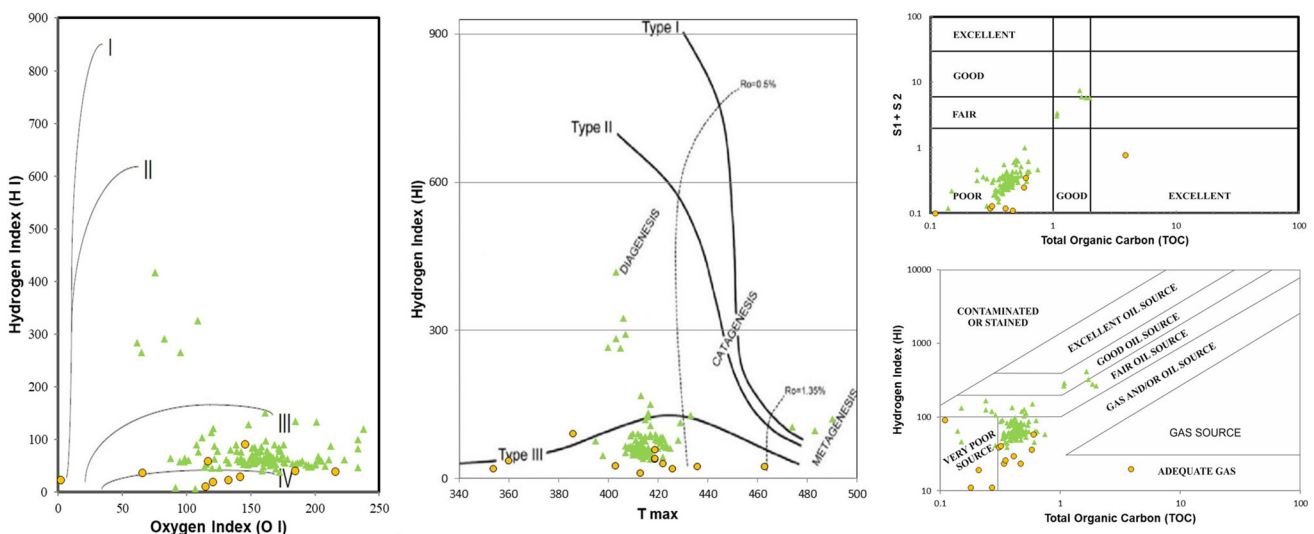


Fig. 7 Plots of the geochemical results. Orange cycles: Miocene surface samples taken in the context of the current study. Green triangles: Published geochemical analyses of surface or ditch cutting samples from the Miocene succession in Messara basin from [5–7]

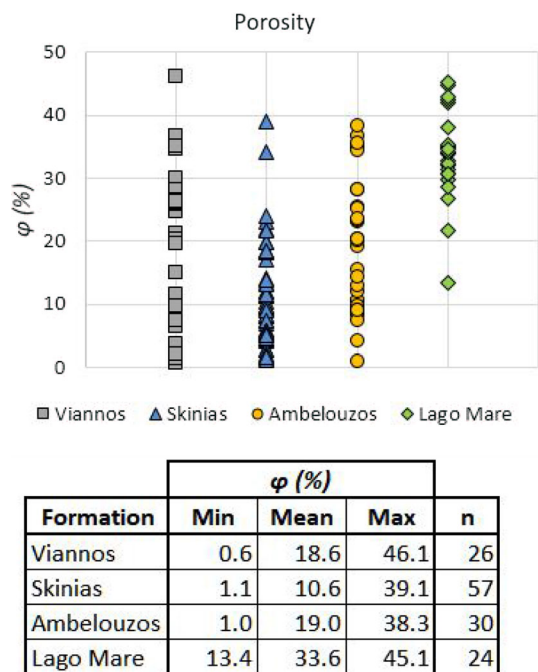


Fig. 8 Porosity distribution per stratigraphic formation

marine deposits of the Ambelouzos formations. The high porosity values of the “Lago Mare” deposits are explained by the marly nature of the deposits which usually show high porosity but small permeability values (low interconnection of the pores’ space).

The correlation between permeability and porosity is usually illustrated on poro/permeability diagrams. Typically, higher porosity values result in better permeability because more pore volume gives more or larger flow paths. In the case that this is not the case, the explanation should be found on factors like the way the pore volume is interconnected, the lithological composition of the rock, the depositional environment, the diagenetic events.

The poro/permeability plots are useful to define different poro/permeability groups representative of different reservoir rock types. Such a grouping has been made on the available 25 samples (Fig. 9). Two different trends can be drawn on this dataset which lead consequently into 2 poro/permeability Groups. The definition of the Groups was based on the rule that each of the Groups should not exceed 2 or a maximum of 3 orders of magnitude in permeability. Group#1 is characterized by poor permeability values ranging from 1mD down to 0.01mD. Most of the “Lago Mare” and Skinias samples belong to this Group. Typically, both formations are characterized by marly/clayey sand lithologies. The nature of these lithologies could explain the higher porosity values and, at the same time, the lower permeability values. The porosity network usually lies in the microporosity range, which does

not favor an extensive pore interconnection. Group#2 is characterized by higher permeabilities (> 1mD) which reach up to approximately 30mD, with good porosity ranges, indicative of good porous rock. Most of the samples in this Group belong to the Ambelouzos formation, which comprises terrestrial to shallow-water sandstones.

4 Discussion

4.1 Messara Subsurface Structure

The seismic lines discussed in this paper provide an insight into the Messara basin’s subsurface structure. The seismic interpretation shows that the Messara basin is separated into three parts: western, central, and eastern. The separation is due to the existence of two subsurface basement highs (Fig. 3, Fig. 10). Both eastern and western parts comprise the greatest depths, while the central part is approximately 400 m shallower. The two basement highs reach to such shallow depths that the seismic can hardly image the strong and continuous reflector identical to the Top surface of the pre-Neogene basement. Therefore, seismic on those highs have a rather chaotic character.

The seismic lines’ coverage does not extend until the alpine basement outcrops, so we cannot set the basin boundaries with certainty. In such a case, surface geology was used to extend the seismic information. Specifically for the eastern part, the basement gets gradually shallower beyond lines 2 and 3. This is because the basement crops out toward to the East and to the North (Dikti Mountains, Fig. 1) and that the northern boundary of Messara basin is the nearby Central Herakleion Ridge which separates Messara from Herakleion basins [29, 51, Fig. 1]. Therefore, the deepest part of the basin that the seismic line 3 covers is at around 1 s TWT (Fig. 3). Using a typical average velocity for the Miocene clastic deposits at 3000 m/s [67], the deepest part is calculated to be around 1500 m. This is consistent with the 1400 m of cumulative vertical motion from Tortonian to Messinian time span estimated by Zachariasse et al. (2011) [51]. The basin depocenters in this area have accommodated the deposition of the largest portion of the Neogene succession. Since both Viannos and Skinias formations comprise the organic-rich sediments, this part of the basin has a significant potential to generate shallow gas (Fig. 4).

4.2 Tectonic Activity

The two major bounding faults, to the South and the West, were activated after the deposition of the two formations. The wedge-like shape of Ambelouzos formation shown in Line 2 on the southern end of the seismic section, suggests syn-tectonic deposition of Ambelouzos formation. The activation

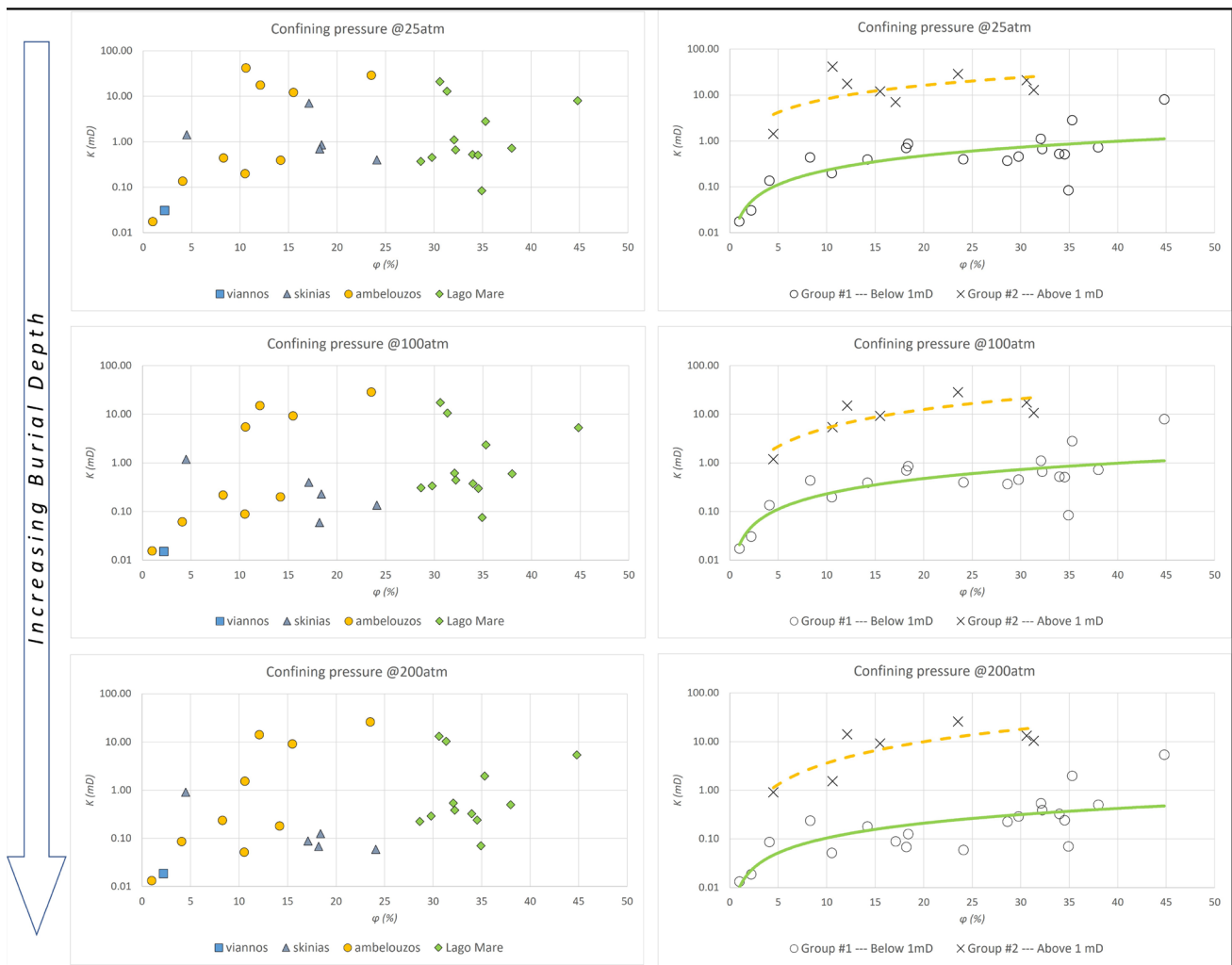


Fig. 9 Poro/permeability diagrams of outcrop samples in Messara basin (for location see Fig. 1). From top to bottom, the graphs illustrate the porosity and permeability values measured under the three different confining pressures of 25, 100, and 200 Atm, respectively. In the left column, the

samples are color-coded as per the lithostratigraphic unit they belong to, while in the right column, the samples are grouped into two poro/permeability types

of these major bounding faults should be regarded as part of the fragmentation event of the Messara basin that started during the last phase of the Skinias deposition 9.7 – 9.6 Ma ago [49]. According to Zachariasse et al. [51], until this time Messara basin had a uniform deposition throughout the basin. The eastern part of the basin continued to subside during the extensional event, whereas the central part of the basin did not, resulting in greater thicknesses of sediment in the eastern part of the basin.

The situation is quite different for the western part. The seismic coverage is inadequate to make an estimate on the maximum depth. Seismic line 11 (Fig. 3) shows that at the western-most edge of the seismic line (where Tymbaki sub-basin is located) normal (or even transtensional) faulting has significantly deepened the basin to the west. Those faults

should be related to the 070 transtensional fault patterns observed in the Messara basin [41] which have generated the Faistos Horst in the same area, which is a pronounced topographic anomaly at the surface of Miocene formations (Fig. 1). Faistos Horst has been documented as being the hydrogeological barrier in between the Tymbaki hydrological basin to the West and the rest of the Messara basin to the East [11]. Near-surface geophysical surveys, water-well data and seismic data covering the Tymbaki sub-basin show a general deepening trend of the basement toward the offshore [76–79].

In the central part of the basin, an extensional regime resulted in basement subsidence, giving space for the Miocene sediments to be deposited. However, the pronounced basement high that separates the central from the

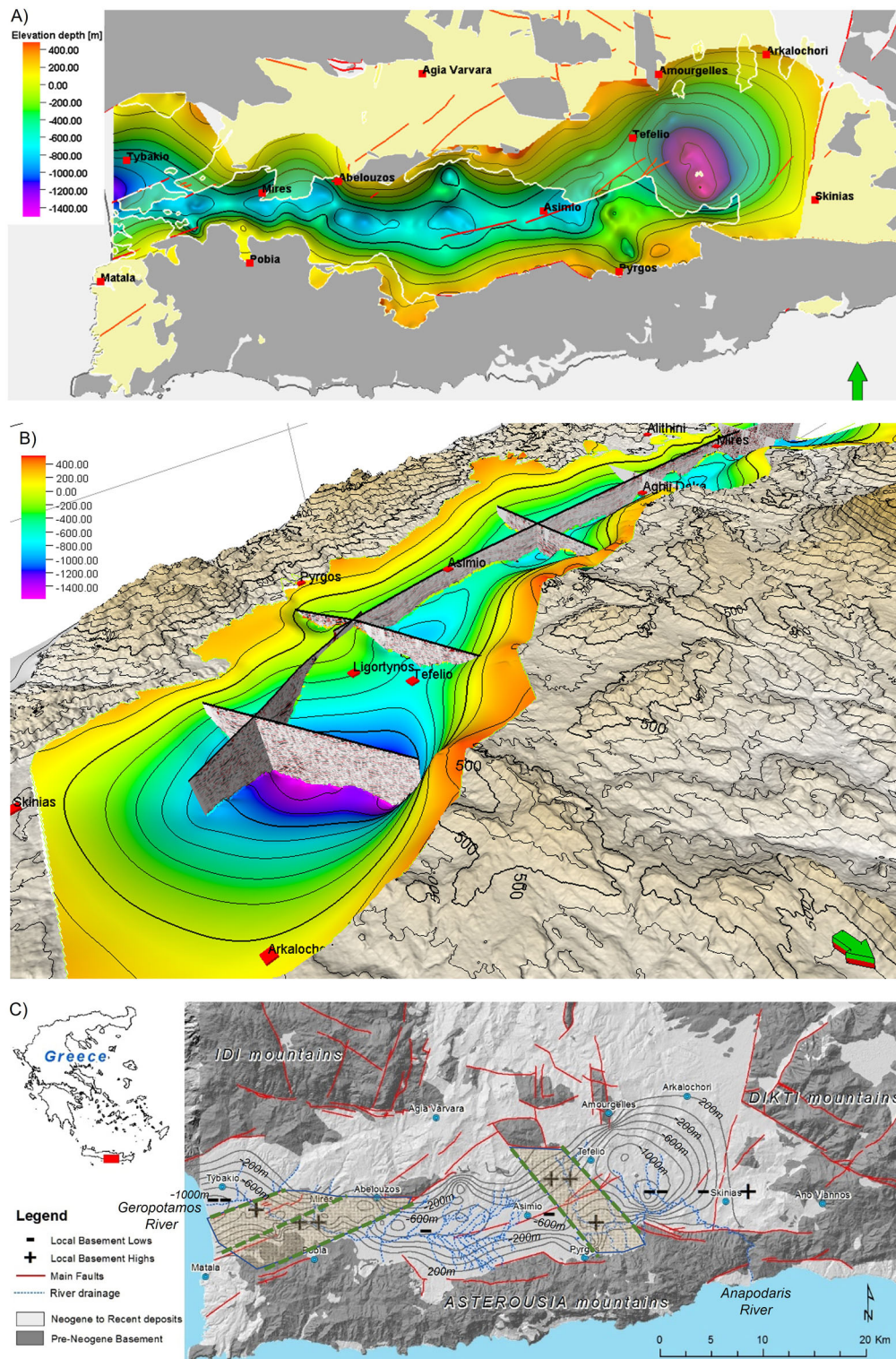


Fig. 10 a The colored-scale structural map of the pre-Neogene basement as resulted from seismic interpretation. The surface exposure of the basement is colored in gray. In pale transparent yellow, are the areas where the Neogene sediments outcrop. The area that is covered by the recent-most sediments is left uncolored. **b** Perspective view toward the

WSW of the subsurface alpine basement, along with the topographic relief. **c** Structural map of the basement (Isodepth contours of the alpine Basement in absolute depth). The shaded areas correspond to the subsurface highs of the basement, which separate the Messara basin into three distinct parts (seismic section in Fig. 3)

eastern part of the basin suggests an early (Miocene?) basin fragmentation. Unfortunately, there are no data for the age of the oldest sediment that has been deposited on the central part of the basin. The basin fragmentation has been overprinted by several transpressional faults patterns generating pop-up structures as shown on the central part of seismic Line 1 (Fig. 3) and Line 6 (Fig. 4). The transpression has deformed both the basement and the overlying Miocene sediments. The Miocene sediments appear to be conformably uplifted over the basement, indicating that the transpression should have happened at least after the deposition of the oldest Miocene sediments (Viannos Formation) in this section. Moreover, van Hinsbergen and Meulenkamp [36] suggest that transpression started during the deposition of Skinias formation (after 10 Ma).

In the late Miocene oblique movements were present due to the Aegean Arc curvature [34, 36]. A left-lateral transpressional regime was suggested to explain the large open folds existing in Crete [36]. The regional strike-slip tectonics that characterizes the southeastern part of the Hellenic Arc since Pliocene has generated a general array of transtensional (e.g., Ptolemy, Pliny, and Strabo troughs) and transpressional structures. These structures influenced the structural evolution of the central part of Messara basin since Pliocene [42 and references therein].

This recent tectonic pattern is aligned to the one that characterizes the SE Aegean region. The stress field is mainly extensional in an NNE–SSW direction combined with considerable strike-slip motions as defined from earthquake slip vectors and geodetically determined horizontal motions [80]. The same authors also suggested four different seismic zones that are highly oblique to the overall Aegean–Anatolia convergence, suggesting partitioning strain into strike-slip and normal components. In fact, the NNE–SSW trend is also justified by focal mechanisms on the onshore central Herakleion [45]. In the Herakleion basin, the epicenter cluster trends NNE–SSW, while in Messara Basin two clusters have been identified trending NE–SW in the northwestern part and N–S in the central part. The epicenter distribution in the onshore area shows that most of the seismic activity is concentrated along the eastern margin of the Heraklion Basin and in the Messara graben to the South. The fault plane solutions in the onshore area indicate both normal and reverse motion and, in some cases, significant horizontal slip component [45]. We, therefore, interpret the compressional structures interpreted on seismic belonging to the same context of this transpressional regime.

4.3 Biogenic Gas Accumulations

The existence of shallow gas in the Messara basin has been identified by the several gas seepages in the area (Fig. 1). According to the available geochemical analyses, those gases

are characterized as biogenic [4–6]. However, no integrated study has been conducted so far to evaluate efficiently the shallow gas potential of the area. The available seismic dataset covers the main part of the basin and broadly reveals the subsurface extent of the Neogene deposits. The seismic interpretation presented in this paper shows that the depocenter of the basin in the eastern area of Messara. This depocenter is covered by approximately 1500 m thick Neogene sediments.

The great thickness that the Neogene deposits have in this part of the basin could also indicate that more organic-bearing layers also exist in the same area. This assumption is supported by the fact that the location of the wells that have encountered gasses are few kilometers to the N/NNW of the depocenter (Fig. 1). The general dip angle/direction of the Neogene strata is 20° – 25° to the S/SSE [66], suggesting that any gas generated in the thicker part of the basin has possibly followed an up-dip fairway to charge the water-wells to the NNW area of the depocenter (Fig. 11). The geochemical analyses of samples taken from Vianos and Skinias formations from the same area have proved the existence of source rock in the area, which is however of fair to poor quality. The capability of this kind of source rocks to generate large quantities of gas cannot be assessed with the current data. Further studies and thermal basin modeling are recommended to evaluate the gas generation potential of the Messara basin.

Considering the fair source rocks quality, an additional scenario to explain the gas shows could be the existence of shale gas. The gas is generated in the fine-grained sediments and remains absorbed. This scenario favors the cases where significant portions of shaley sections exist, as is the case in well D (Fig. 6). However, since there is no information to define which were the well intervals that have given the gas, there is no definite answer on whether the Neogene succession in Messara hosts conventional gas or shale-gas, or even a hybrid. Moreover, the existence of coals in the Viannos and Ambelouzos formation [34, 50] could also be an additional source of the gas. The coal beds, however, seem to be localized rather being extensive throughout the basin and therefore are regarded as to have a limited contribution in the gas generation.

Regardless of the source quality and the gas quantities, the proposed concept suggest that the gas migrates from the deeper part of the basin and accumulates into the coarse-grained sediments following the sediments layering and facilitated from the existence of fault zones (Fig. 11). The alternations of fine-grained and coarse-grained sediments in the whole Miocene succession [34, 36, 50] provide an efficient stratigraphic trapping mechanism.

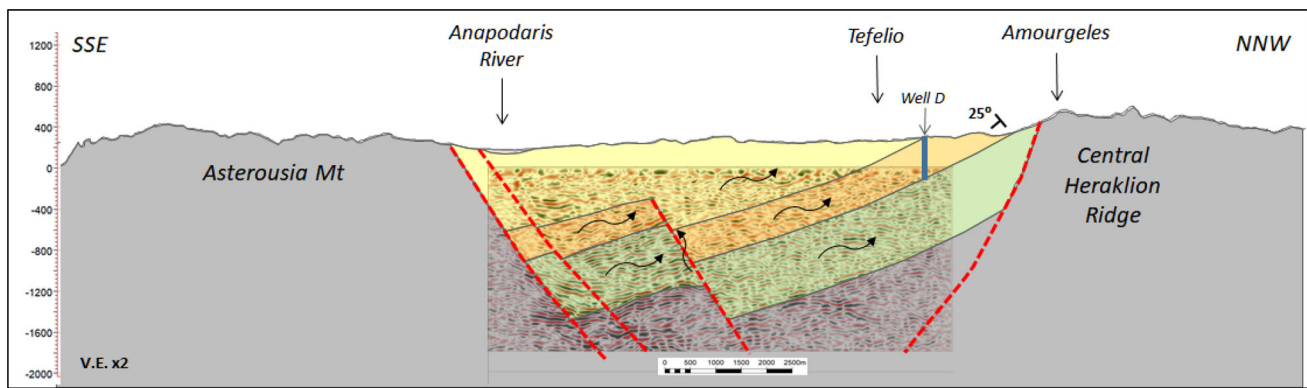


Fig. 11 Geoseismic section along seismic Line 2 illustrates a simplified concept for explaining the gas shows in Well-D (Well-D is projected 1 km on the section). According to this concept, the great thickness of the Neogene deposits around the basin depocenter and the greater

depth that the organic-bearing Viannos (colored green) and Skinias formations (colored orange) have reached, could have generated the gas which migrates to the NNW following the bed strata and the faults and observed on the water wells (such as Well-D). Vertical scale in meters exaggerated $\times 2$

4.4 A Potential Play in the Area Between the Tymbaki Sub-basin and Gavdos

The insufficient seismic coverage in the western part of the basin, the so-called Tymbaki sub-basin, and the poor quality of line 11 do not help in picking the basement on seismic with confidence. However, a deepening trend of the basement can be inferred from seismic sections. The deepening trend is also observed on the Top-Miocene Horizon, as derived by shallow well and geophysical data in Tymbaki [78, 79]. In the offshore area on the Gulf of Messara, the pre-Neogene basements keep getting deeper, creating a trench in between the south coasts of Crete and the island of Paximadia in the Gulf of Messara [76, 77]. The Neogene deposits are found in even greater depths beyond the Paximadia islands [77, 81, 82]. Following this deepening trend, a fair assumption can be drawn that the organic-rich sediments sitting in this area may have possibly reached the maturation depths.

Even though the Neogene sediments in this area are laterally equivalent to the ones in the onshore area of Messara, the depositional environment seems to be different compared to Messara basin, as during Serravallian-Tortonian period the area of Tymbaki sub-basin was a transition zone in between the fluvio-lacustrine deposits in central Crete and the deep marine deposits in Gavdos Island [36]. Consequently, this type of data demonstrates that the Tymbaki sub-basin has a slightly different evolutionary history compared to the rest of the Messara basin, which might also support the existence of a different hydrocarbon play. In fact, the geochemical analysis of Tortonian samples located further to the SW in Gavdos Island have given higher TOC values, but still thermally immature [73]. It is therefore suggested that the area in between the Tymbaki sub-basin and the Gavdos island

hosts organic-rich sediments which could have been buried in greater depths, possibly entering the oil window [53, 73].

5 Conclusions

This paper describes the subsurface structure of the Messara basin which is divided into three distinct parts. The western and the eastern parts exhibit the greatest depths, while the central part is significantly more elevated. The depocenter of the east part is approximately 1 s TWT covered by Miocene clastic sediments. Regarding the western part of the basin, the basement gets significantly deeper west of Faistos Horst. The limited seismic data the deepest part that has been mapped is approximately 1 km below sea level in the Western depocenter and 1.4 km in the Eastern.

The seismic lines reveal the complicated multi-phased tectonic history of the Messara basin. The first phase is characterized by extension which resulted in creating the accommodation space for the Miocene sediments. The second one is a compressional phase affecting mainly the central part of the basin, which deformed both the basement and the Miocene sediments. The timing of the second event seems to be during the latest stage of the deposition of the Neogene sediments.

The inverse activation of the pre-existing bounding normal faults in the central part of the basin has formed pop-up structures. Such structures are part of the regional strike-slip tectonics acting in the southeastern edge of the Hellenic Arc which has also formed similar structures in the area (i.e., Ptolemy, Pliny, and Strabo trenches).

The gas shows have been encountered on water-wells located at the eastern part of the Messara basin, where the deeper part of the basin has been identified on seismic. The

1500 m thick organic-bearing Miocene sediments are suggested to act as the source for the observed biogenic gas. The gas migration follows the general dip direction of the Miocene strata charging the sediments located in the area to the NNW of the basin depocenter. The gas accumulates into good porosity sandstones trapped by the vertical and lateral alternations with claystones and marls.

Given that the Miocene basin was extended to the area south of Crete, a hypothetical play can be argued for the Tymbaki sub-basin following similar assumptions like in the Messara basin in terms of source, reservoir, and trapping mechanism. The Tymbaki sub-basin is probably part of a petroleum system extended up to Gavdos island. The source rocks are expected to be buried in greater depths in the area between Gavdos and Tymbaki.

It is recommended that additional studies should be carried out to describe the gas play of the eastern part of the Messara basin, as well as, to explore the existence of any working hydrocarbon system in the offshore area between Tymbaki sub-basin and Gavdos island.

Acknowledgements This study has not been supported by a funding program. Prof. Pantelis Soupios is supported by the start-up fund (SF18063), College of Petroleum Engineering and Geosciences (CPG), KFUPM. This paper presents data as part of the Ph.D. research that Mr. George Panagopoulos is currently carrying out in the Technical University of Crete. The authors would like to thank the Greek Ministry of Environment and Energy for providing us with the seismic data and permitting us to publish them. The seismic data were interpreted in Petrel by using one of the licenses which Schlumberger donated to the School of Mineral Resources Engineering of the Technical University of Crete. The reprocessing of the seismic data was performed on the “Laboratory of Applied Geophysics”. The laboratory analyses (porosity, permeability, TOC) were performed with the equipment of the “Laboratory of PVT and Core Analysis” and “Hydrocarbons Chemistry and Technology” of the Technical University of Crete. Many thanks to Prof. Nikolaos Pasadakis for his review on the geochemical results and Prof. Avraam Zelilidis for his fruitful comments and for the fieldwork done in the beginning of this study. Finally, the authors would like to thank the 3 anonymous reviewers, who improved the final version of the manuscript with their comments.

Declarations

Conflict of Interest The authors declare no conflict of interest.

Open Access This article is licensed under a Creative Commons Attribution 4.0 International License, which permits use, sharing, adaptation, distribution and reproduction in any medium or format, as long as you give appropriate credit to the original author(s) and the source, provide a link to the Creative Commons licence, and indicate if changes were made. The images or other third party material in this article are included in the article’s Creative Commons licence, unless indicated otherwise in a credit line to the material. If material is not included in the article’s Creative Commons licence and your intended use is not permitted by statutory regulation or exceeds the permitted use, you will need to obtain permission directly from the copyright holder. To view a copy of this licence, visit <http://creativecommons.org/licenses/by/4.0/>.

References

- Smil, V.: Natural gas: fuel for the 21st century Wiley. Hoboken, New Jersey (2015)
- Hayhoe, K.; Khesghi, H.S.; Jain, A.K.; Wuebbles, D.J.: Substitution of natural gas for coal: climatic effects of utility sector emissions. *Climatic Change* **54**, 107–139 (2020). <https://doi.org/10.1023/A:1015737505552>
- IPCC: Climate change 2007: synthesis report. contribution of working groups I, II and III to the fourth assessment report of the Intergovernmental Panel on Climate Change, Geneva, Switzerland (2007)
- Pasadakis, N.; Manoutsoglou, E.; Zelilidis, A.; Lic, M.: Source rock geochemical study of shallow biogenic methane accumulations in Crete (Greece) island. 24th International Meeting on Organic Geochemistry. September 6–11, Bremen, Germany, 466 (2009)
- Pasadakis, N.; Dagounaki, V.; Chamilaki, E.; Vafeidis, A.; Zelilidis, A.; Piliotis, I.; Panagopoulos, G.; Em, Manoutsoglou: Organic geochemical evaluation of neogene formations in Messara (Herackion, Crete) basin as source rocks of biogenetic methane. *Mineral Wealth* **166**, 7–26 (2012)
- Maravelis, A.; Panagopoulos, G.; Piliotis, I.; Pasadakis, N.; Manoutsoglou, E.; Zelilidis, A.: Pre-Messinian (sub-salt) source-rock potential on back-stop basins of the hellenic trench system (Messara Basin, Central Crete, Greece). *Issue Oil Gas Sci. Technol. – RevIFP Energies nouvelles* **71**, 1–16 (2016)
- Kontakiotis, G.; Karakitsios, V.; Cornée, J.; Moissette, P.; Zarkogiannis, S.; Pasadakis, N.; Koskeridou, E.; Manoutsoglou, E.; Drinia, H.; Antonarakou, A.: Preliminary results based on geochemical sedimentary constraints on the hydrocarbon potential and depositional environment of a Messinian sub-salt mixed siliciclastic-carbonate succession onshore Crete (Plouti section, eastern Mediterranean). *Mediterranean Geosci. Rev.* **2**, 247–265 (2020)
- FAO: Greece: geophysical survey performed in Messara plain (Eastern Crete). Final report. Fondazione Ing. C. M. Lerici Del Politecnico, Milan, Italy (1969)
- FAO: Study of the water resources and their exploitation for irrigation in eastern Crete – Greece. Drillings and pumping tests in Messara AGL:SF/GRE 17/31 tech. rep. 26, UNDP, Iraklio (1972)
- Paritsis, S.N.: Simulation of seawater intrusion into the Tymbakion aquifer, South Central Crete, Greece. Report within MEDIS project, Study implemented on behalf of the Department of Management of Water Resources of the Region of Crete. Heraklion, Crete, Greece. (2005)
- Kritsotakis, M.; Tsanis, I.K.: An integrated approach for sustainable water resources management of Messara Basin, Crete. *Greece. European Water* **27–28**, 15–30 (2009)
- Vafidis, A.; Andronikidis, N.; Economou, N.; Panagopoulos, G.; Zelilidis, A.; Manoutsoglou, E.: Reprocessing and interpretation of seismic reflection data at Messara Basin, Crete, Greece. *J. Balkan Geophys. Soc.* **15**(2), 31–40 (2012)
- Alves, T.; Cupkovic, T.: Footwall degradation styles and associated sedimentary facies distribution in SE Crete: insights into tilt-block extensional basins on continental margins. *Sed. Geol.* **367**, 1–19 (2018)
- Makris, J.: A Geophysical Study of Greece based on Deep Seismic Studies, Gravity and Magnetism. in Alps, Appenines, Hellenides (ed. H.Closs, D.Roeder, K.Schmidt): 415–423, Stuttgart Schweitzerbartsche Verlagsbuchhandlung. (1978)
- Le Pichon, X.; Angelier, J.: The Hellenic arc and Trench system: a key to the neotectonic evolution of the eastern Mediterranean area. *Tectonophysics* **60**, 1–42 (1979)
- Meulenkamp, J.E.; Wortel, M.J.R.; Van Wamel, W.A.; Spakman, W.; Hoogerduyn Starting, E.: On the Hellenic subduction zone



- and the geodynamic evolution of Crete since the late Middle Miocene. In: F.-C. Wezel (Editor). *The Origin and Evolution of Arcs*. Tectonophysics, 146, 203–215 (1988)
17. Jackson, J.: Active tectonics of the Aegean Region. *Annu. Rev. Earth Planet. Sci.* **22**, 239–271 (1994)
 18. Le Pichon, X.; Chamot-Rooke, N.; Lallemand, S.: Geodetic determination of the kinematics of central Greece with respect to Europe: implications for eastern Mediterranean tectonics. *J. Geophys. Res.* **100**, 12675–12690 (1995)
 19. McKenzie, D.P.: Plate tectonics of the Mediterranean region. *Nature* **226**, 239–243 (1970)
 20. Peterek, A.; Schwarze, J.: Architecture and late pliocene to recent evolution of outer-arc basins of the Hellenic subduction zone (south-central Crete, Greece). *J. Geodyn.* **38**, 19–55 (2004)
 21. Fassoulas, C.; Kiliyas, A.; Mountrakis, D.: Post-nappe stacking extension and exhumation of the HP/LT rocks in the island of Crete, Greece. *Tectonics* **13**, 127–138 (1994)
 22. Bonneau, M.: Correlation of the Hellenic Nappes in the South-East Aegean and their tectonic reconstruction. In: J. E. Dixon & A. H. F. Robertson (eds.) *The Geological Evolution of the Eastern Mediterranean* (Ed. by), Geol. Soc., Lond., Spec. Publ., 17, 517–527 (1984)
 23. Chatzaras, V.; Xypolias, P.; Kokkalas, S.; Koukouvelas, I.: Tectonic evolution of a crustal-scale oblique ramp, Hellenides thrust belt, Greece. *J. Struct. Geol.* **57**, 16–37 (2013). <https://doi.org/10.1016/j.jsg.2013.10.003>
 24. Creutzburg, N.; Seidel, E.: Zum stand der geologie des präneogens auf kreta. *Neues. Jb. Geol. Paläont. Abh.* **149**, 363–383 (1975)
 25. Bonneau, M.: Geological Map of Greece, Achantrias sheet, scale 1:50.000, Greek Geological Survey (I.G.M.E.), Athens (1984)
 26. Seidel, M.; Seidel, E.; Stockhert, B.: Tectono-sedimentary evolution of lower to middle Miocene half-graben basins related to an extensional detachment fault (western Crete, Greece). *Terra Nova* **19**, 39–47 (2007)
 27. Papanikolaou, D.; Vassilakis, E.: Thrust faults and extensional detachment faults in Cretan tectono-stratigraphy: implications for middle miocene extension. *Tectonophysics* **488**, 233–247 (2010)
 28. Creutzburg, N.; Drooger, C.W.; Meulenkamp, J.E.: Geological Map of Crete: Athens, scale 1:200.000, Greek Geological Survey (I.G.M.E.), Athens (1977)
 29. Kiliyas, A.; Sotiriadis, L.; and Mountrakis, D.: New data concerning the structural geology of Western Crete. The transgressive carbonate mass of the Herospilion Area Geological and Geophysical Research, Special Issue: Greek Geological Survey (I.G.M.E.), 213–223, Athens (1985)
 30. Kröger, K.; Brachert, T. C.; Reuter, M.: The Sedimentary History of Southern Central Crete: Implications for Neogene Uplift. EGS - AGU - EUG Joint Assembly, Nice, France, 10375 (2003)
 31. Angelier, J.; Lybéris, N.; Pichon, X.L.; Barrier, E.; Huchon, P.: The tectonic development of the Hellenic arc and the Sea of Crete: a synthesis. *Tectonophysics* **86**, 159–196 (1982)
 32. Duermeijer, C.E.; Krijgsman, W.; Langereis, C.G.; Ten Veen, J.H.: Post-early Messinian counterclockwise rotations on Crete: implications for late miocene to recent kinematics of the southern Hellenic arc. *Tectonophysics* **298**, 177–189 (1998)
 33. Ten Veen, J.H.; Meijer, P.H.: Late miocene to recent tectonic evolution of Crete (Greece): geological observations and model analysis. *Tectonophysics* **298**, 191–208 (1998)
 34. Ten Veen, J.H.; Postma, G.: Neogene tectonics and basin fill patterns in the Hellenic outer-arc (Crete, Greece). *Basin Res.* **11**, 243–266 (1999)
 35. Fassoulas, C.: The tectonic development of a Neogene basin at the leading edge of the active European margin: the Heraklion basin, Crete, Greece: *Journal of Geodynamics* **31**, 49–70 (2001)
 36. van Hinsbergen, D.J.J.; Meulenkamp, J.E.: Neogene supra-detachment basin development on Crete (Greece) during exhumation of the South Aegean core complex. *Basin Res.* **18**, 103–124 (2006)
 37. Jolivet, L.; Goff, B.; Moni, P.; Truffert-Luxey, C.; Patriat, M.; Bonneau, M.: Miocene detachment in Crete and exhumation P-T-t paths of high-pressure metamorphic rocks. *Tectonics* **15**(6), 1129–1153 (1996)
 38. Zachariasse, W.J.; van Hinsbergen, D.J.J.; Fortuin, A.R.: Mass wasting and uplift on Crete and Karpathos during the early Pliocene related to initiation of South Aegean left-lateral, strike-slip tectonics. *Geol. Soc. Am. Bull.* **120**, 976–993 (2008)
 39. Meulenkamp, J.E.; van der Zwaan, G.J.; van Wamel, W.A.: On late miocene to recent vertical motions in the Cretan segment of the Hellenic arc. *Tectonophysics* **234**, 53–72 (1994)
 40. Kokkalas, S.; Doutsos, T.: Strain-dependent stress field and plate motions in the south-east Aegean region. *J. Geodyn.* **32**, 311–332 (2001)
 41. Ten Veen, J.H.; Kleinspehn, K.L.: Incipient continental collision and plate-boundary curvature: late Pliocene Holocene transtensional Hellenic forearc, Crete, Greece. *J. Geol. Soc. London* **160**, 161–181 (2003)
 42. Sakellariou, D.; Tsampouraki-Kraounaki, K.: Plio-Quaternary extension and strike-slip tectonics in the Aegean. In: J. Duarte (Ed.): *Transform Plate Boundaries and Fracture Zones*, Chapter 14, 339–374 (2019)
 43. Taymaz, T.; Jackson, J.; Westaway, R.: Earthquake mechanics in the Hellenic Trench near Crete. *Geophys. J. Int.* **102**, 695–731 (1990)
 44. Gallen, S.F.; Wegmann, K.W.; Bohnenstiehl, D.R.; Pazzaglia, F.J.; Brandon, M.T.; Fassoulas, C.: Active simultaneous uplift and margin-normal extension in a forearc high, Crete, Greece. *Earth and Planet. Sci. Lett.* **398**, 11–24 (2014)
 45. Delibasis, N.; Ziazia, M.; Voulgaris, N.; Papadopoulos, T.; Stavrakakis, G.; Papanastassiou, D.; Drakatos, G.: Microseismic activity and seismotectonics of Heraklion area (central Crete Island, Greece). *Tectonophysics* **308**, 237–248 (1999)
 46. Jost, M.L.; Knabenbauer, O.; Cheng, J.; Harjes, H.P.: Fault plane solutions of microearthquakes and small events in the Hellenic arc. *Tectonophysics* **356**, 87–114 (2002)
 47. Pondrelli, S.; Morelli, A.; Ekstrom, G.; Mazza, S.; Boschi, E.; Dziewonski, A.M.: European-Mediterranean regional centroid-moment tensors: 1997–2000. *Phys. Earth planet. Int.* **130**, 71–101 (2002)
 48. Kiratzi, A.; Louvari, E.: Focal mechanisms of shallow earthquakes in the Aegean Sea and the surrounding lands determined by waveform modeling: a new database. *J. Geodyn.* **36**, 251–274 (2003)
 49. Caputo, R.; Catalano, S.; Monaco, C.; Romagnoli, G.; Tortorici, G.; Tortorici, L.: Active faulting on the island of Crete (Greece). *Geophys. J. Int.* **183**, 111–126 (2010)
 50. Meulenkamp, J.E.; Dermitzakis, M.; Georgiadou-Nikeouli, E.; Jonkers, H.A.; Boger, H.: Field guide to the Neogene of Crete. In: N. Symeonidis, D. Papanikolaou & M. Dermitzakis (eds.) *Publications of the Department of Geology and Paleontology, University of Athens. Series A*, 32, 1–32 (1979)
 51. Zachariasse, W.J.; van Hinsbergen, D.J.J.; Fortuin, A.R.: Formation and fragmentation of a late Miocene supradetachment basin in central Crete: implications for exhumation mechanisms of high-pressure rocks in the Aegean forearc. *Basin Res.* **23**(6), 678–701 (2011)
 52. Mantzouka, D.; Kvaček, Z.; Teodoridis, V.; Utescher, T.; Tsaparas, N.; Karakitsios, V.: A new late Miocene (Tortonian) for a from Gavdos Island in southernmost Greece evaluated in the context of vegetation and climate in the Eastern Mediterranean. *Neues Jahrbuch für Geologie und Paläontologie - Abhandlungen* **275**(1), 47–81 (2015). <https://doi.org/10.1127/njgpa/2015/0448>

53. Zelilidis, A.; Tserolas, P.; Chamilaki, E.; Pasadakis, N.; Kostopoulou, S.; Maravelis, A.G.: Hydrocarbon prospectivity in the Hellenic trench system: organic geochemistry and source rock potential of upper Miocene-lower Pliocene successions in the eastern Crete Island, Greece. *Intr. J. Earth Sci.* **105**, 1859–1878 (2016)
54. Zidianiakos, G.; Iliopoulos, G.; Zelilidis, A.; Kovar-Eder, J.: Pinus remains from the Pitsidia plant assemblage document coastal pine forests in southern Crete during the late Miocene. *Rev. Palaeobot. Palynol.* **235**, 11–30 (2016). <https://doi.org/10.1016/j.revpalbo.2016.09.003>
55. Zidianiakos, G.; Iliopoulos, G.; Zelilidis, A.; Kovar-Eder, J.: Three (middle to) late Miocene plant macroremain assemblages (Pitsidia, Kassanoi and Metochia) from the Messara Gavdos region, southern Crete. *Acta Palaeobotanica* **60**(2), 333–437 (2020). <https://doi.org/10.35535/acpa-2020-0018>
56. Espitalié, J.; Laporte, J.L.; Madec, M.; Marquis, F.; Leplat, P.; Paulet, J.; Boutefeu, A.: Méthode rapide de caractérisation des roches mères, de leur potentiel pétrolier et de leur degré d'évolution. *Rev Inst Fr Pét* **32**, 23–42 (1977)
57. Espitalié, J.; Deroo, G.; Marquis, F.: La pyrolyse Rock-Eval et ses applications. Première partie. *Rev Inst Fr Pét* **40**, 73–89 (1985)
58. Tyson, R.V.: Sedimentary organic matter, organic facies and palynofacies. Chapman and Hall, London (1995)
59. Tissot, B.P.; Welte, D.H.: Petroleum formation and occurrence, 2nd edn. Springer, Berlin (1984)
60. Hunt, J.M.: Petroleum geochemistry and geology, 2nd edn. W.H.Freeman and Company, New York (1996)
61. Jones, R.W.: Comparison of carbonate and shale source rocks. In: Palacas JG (ed) Petroleum geochemistry and source rock potential of carbonate rocks, vol 18. AAPG Stud. Geol., Tulsa, 163–180 (1984)
62. Filomena, C.M.; Hornung, J.; Stollhofen, H.: Assessing accuracy of gas-driven permeability measurements: a comparative study of diverse Hassler-cell and probe permeameter devices. *Solid Earth* **5**, 1–11 (2014). <https://doi.org/10.5194/se-5-1-2014>
63. Bonneau, M.; Jonkers, H.A.; Meulenkamp, J.E.: Geological map of Greece, Timbakion sheet, scale 1:50.000, Greek Geological Survey (I.G.M.E.), Athens (1984)
64. Davi, E.; Bonneau, M.: Geological Map of Greece, Antiskari sheet, scale 1:50.000, Greek Geological Survey (I.G.M.E.), Athens (1985)
65. Vidakis, M.; Meulenkamp, J.E.; Jonkers, H.A.: Geological Map of Greece, Mohos sheet, scale 1:50.000, Greek Geological Survey (I.G.M.E.), Athens (1989)
66. Vidakis, M.; Jonkers, H.A.; Meulenkamp, J.E.: Geological Map of Greece, Epano Archanes sheet, scale 1:50.000, Greek Geological Survey (I.G.M.E.), Athens (1994)
67. Kokkalas, S.; Kamperis, E.; Xypolias, P.; Sotiropoulos, S.; Koukouvelas, I.: Coexistence of thin- and thick-skinned tectonics in Zakynthos area (western Greece): Insights from seismic sections and regional seismicity. *Tectonophysics* **597–598**, 73–84 (2012)
68. Shurr, W.G.; Ridgley, L.J.: Unconventional Shallow Biogenic Gas Systems. AAPG (2002)
69. Clayton, C., 1992. Source volumetrics of biogenic gas generation. Bacterial gas: proceedings of the Conference held in Milan, September 25–26 (1989)
70. Rice, D.D.; Claypool, G.: E: Generation, accumulation and resource potential of biogenic gas. *Am. Assoc. Pet. Geol. Bull.* **74**, 1343 (1981)
71. Schoell, M.: Genetic characterization of natural gases: AAPG Bulletin **67**(12), 2225–2238 (1983)
72. Krijgsman, W.; Hilgen, F.J.; Langereis, C.G.; Zachariasse, W.J.: The age of the Tortonian/Messinian boundary. *Earth Planet Sci Lett* **121**, 533–547 (1994)
73. Pyliotis, I.; Zelilidis, A.; Pasadakis, N.; Panagopoulos, G.; Manoutsoglou, E.: Source rock potential of the late Miocene Metochia formation of Gavdos island, Greece. *Bull Geol Soc Greece*, XLVII **2**, 871–879 (2013)
74. Tissot, B.P.; Welte, D.H.: Petroleum Formation and Occurrence. 2nd Edition, Springer-Verlag, Berlin, 699 (1984)
75. Pang, X.; Zhao, W.; Su, A.; Zhang, S.; Li, M.; Dang, Y.; Xu, F.; Zhou, R.; Zhang, D.; Xu, Z.; Guan, Z.; Chen, J.; Li, S.: Geochemistry and origin of the giant quaternary shallow gas accumulations in the eastern Qaidam Basin, NW China. *Org. Geochem.* **36**, 1636–1649 (2005)
76. Karvelis, P.: A contribution to the knowledge of the Hellenic Arc geodynamic regime based on the identification of active faults. University of Athens, Geological department, Phd Thesis, 259 (1996) (in Greek)
77. Kokinou, E.; Alves, T.; Kamberis, E.: Structural decoupling in a convergent forearc setting (southern Crete, Eastern Mediterranean). *Geol. Soc. Am. Bull.* **124**, 1352–1364 (2012)
78. Panagopoulos, G.; Manoutsoglou, E.; Vafidis, A.; Soupios, P.; Bellas, S.: Subsurface Structure of Tympaki Basin (Crete, Greece) based on well and geophysical data. EAGE, proceedings the 8th Congress of Balkan Geophysical Society, Chania, 27176 (2015)
79. Panagopoulos, G.; Soupios, P.; Vafidis, A.; Manoutsoglou, E.: Integrated use of well and geophysical data for constructing 3D geological models in shallow aquifers: a case study at the Tymbakion basin, Crete, Greece. *Environm. Earth Sci.* **80**, 142 (2021). <https://doi.org/10.1007/s12665-021-09461-5>
80. Kokkalas, S.; Aydin, A.: Is there a link between faulting and magmatism in the south-central Aegean Sea? *Geol. Mag.* **150**(2), 193–224 (2013)
81. Alves, T.M.; Lykousis, V.; Sakellariou, D.; Alexandri, S.; Nomikou, P.: Constraining the origin and evolution of confined turbidite systems: Southern Cretan margin, Eastern Mediterranean Sea (34°30–36°N). *Geo-Marine Lett* **27**, 41–61 (2007). <https://doi.org/10.1007/s00367-006-0051-1>
82. Manta, K.; Rousakis, G.; Anastasakis, G.; Lykousis, V.; Sakellariou, D.; Panagiotopoulos, I.P.: Sediment transport mechanisms from the slopes and canyons to the deep basins south of Crete Island (southeast Mediterranean). *Geo-Mar. Lett.* **39**, 295–312 (2019). <https://doi.org/10.1007/s00367-019-00575-1>

